# A New Hexagonal 12-Layer Perovskite-Related Structure: $Ba_6R_2Ti_4O_{17}$ (R = Nd and Y)

Xiaojun Kuang,[†] Xiping Jing,*[,†] Chun-K. Loong,[‡] Eric E. Lachowski,[§] J. M. S. Skakle,[§] and Anthony R. West[||]

*State Key Laboratory of Rare Earth Materials Chemistry & Application, College of Chemistry and Molecular Engineering, Peking University, Beijing 100871, P. R. China, Intense Pulse Neutron Source Division, Argonne National Laboratory, Argonne, Illinois 60439, Department of Chemistry, University of Aberdeen, Aberdeen AB24 3UE, U.K., and Department of Engineering Materials, University of Sheffield, Sheffield S1 3JD, U.K.*

*Received May 13, 2002. Revised Manuscript Received July 29, 2002*

The crystal structure of $Ba_6R_2Ti_4O_{17}$ (R = Nd and Y) was determined by combined analysis of X-ray and neutron powder diffraction data. Both materials crystallize in hexagonal symmetry with space group $P6_3/mmc$, $Z = 2$. The unit cell parameters at room temperature are $a = 5.99283(9)$ Å and $c = 29.9289(8)$ Å for Nd and $a = 5.93055(4)$ Å and $c = 29.5239(3)$ Å for Y. The structure can be described as stacking of cubic (c) and hexagonal (h) [$BaO_3$] layers as well as ordered, oxygen-deficient, pseudo-cubic (c′) [$BaO_2$] layers in the sequence of $(c'cchcc)_2$ along the *c*-axis and belongs to the 12-layer hexagonal perovskite-related family. The structural framework exhibits face-sharing $TiO_6$ octahedral layers ($Ti_2O_9$), $RO_6$ octahedral layers, and $TiO_4$ tetrahedral layers. The $TiO_4$ subunits form around the c′ layers.

## 1. Introduction

Compounds belonging to the perovskite family exhibit a rich variety of remarkable physical properties, ranging from high-$T_c$ superconductivity[1] to colossal magnetoresistance,[2] high permittivity at microwave frequencies,[3] and oxygen-ion conduction.[4] These fundamental materials properties as well as potential technological applications have promoted numerous studies over many decades in the fields of solid-state physics and chemistry.[2−6]

It is well-known that the structure of hexagonal perovskites $ABO_3$ can be constructed by stacking cubic (c) corner-sharing octahedra and hexagonal (h) face-sharing octahedral; close-packed [$AO_3$] layers sandwich B atoms in octahedral sites to form $BO_6$ octahedra. Along the crystallographic *c* direction, the c and h layers are stacked alternately. In the typical hexagonal perovskite $BaTiO_3$,[7] the stacking sequence along the *c* axis is $(cch)_2$, which consists of 6 layers of $TiO_6$ octahedra. In hexagonal perovskites and related structures, the ratio and the stacking sequence of c and h layers are influenced by various factors, such as the ionic sizes, electronegativity, and valence of the elements.[7−10] Some hexagonal perovskite-related compounds form oxygen-deficient phases $ABO_{3-\delta}$, induced by mixed valency of the A-site and/or B-site elements. In these phases, oxygen-deficient cubic (c′) [$BaO_2$] layers may appear, such as in $BaCoO_{2.6}$[8] and $Ba_4Ca_{1-x}Mn_{3-x}O_{12-\delta}$.[9] The former has a 12-layer structure with the stacking sequence $(c'chhhc)_2$ and the latter exhibits a 16-layer structure with the sequence $(hhhccc'cc)_2$.

During a study of the $TiO_2$-rich region of the BaO−$Nd_2O_3$−$TiO_2$ system, Kolar et al.[11] discovered two phases, $BaNd_2Ti_3O_{10}$ and $Ba_{6-3x}Nd_{8+2x}Ti_{18}O_{54}$, both of which have perovskite-related structures. Subsequent studies showed that $BaNd_2Ti_3O_{10}$ forms a monoclinic Ruddlesden−Popper layer structure ($(AO)_m(ABO_3)_n$, *m* and *n* are integers) with $n = 3$, that is, $(Ba_{1/2}O)$-$(Ba_{1/2}TiO_3)(NdTiO_3)_2$,[12] and $Ba_{6-3x}Nd_{8+2x}Ti_{18}O_{54}$ has an orthorhombic tungsten bronze structure containing $3 \times 3$ octahedra units of cubic perovskite.[13] The latter material has good microwave dielectric properties (permittivity $\epsilon \approx 85$, dielectric loss $\tan \delta \approx 0.00025$ and temperature coefficient of resonate frequency $\tau_f \approx 0$ ppm/°C at 3 GHz[14]).

During a study of the ternary system BaO−$Nd_2O_3$−$TiO_2$, we identified a new phase, labeled as $Q_1$, with a

* To whom correspondence should be addressed. E-mail: xpjing@chem.pku.edu.cn.
[†] Peking University.
[‡] Argonne National Laboratory.
[§] University of Aberdeen.
[||] University of Sheffield.

(1) Bednorz, J. G.; Müller, K. A. *Z. Phys.* **1986**, *B64*, 189.
(2) Ibarra, M. R.; Teresa, J. M. De *J. Magn. Magn. Mater.* **1998**, *177−181*, 846.
(3) Vineis, C.; Davies, P. K.; Negas, T.; Bell, S. *Mater. Res. Bull.* **1996**, *31* (5), 431.
(4) Skinner, S. J. *Int. J. Inorg. Mater.* **2001**, *3*, 113.
(5) Raveau, B.; Michel, C.; Hervieu, M.; Groult, D.; Provost, J. *J. Solid State Chem.* **1990**, *85*, 181.
(6) Darriet, J.; Subramanian, M. A. *J. Mater. Chem.* **1995**, *5* (4), 543.
(7) Burbank, R. D.; Evans, H. T. *Acta Crystallogr.* **1948**, *1*, 330.
(8) Jacobson, A. J.; Hutchinson, J. L. *J. Solid State Chem.* **1980**, *35*, 334.
(9) Floros, N.; Michel, C.; Hervieu, M.; Raveau, B. *Chem. Mater.* **2000**, *12* (10), 3197.
(10) Liu, G.; Greedan, J. E. *J. Solid State Chem.* **1994**, *108*, 371.
(11) Kolar, D.; Gaberscek, S.; Volavsek, B. *J. Solid State Chem.* **1981**, *38*, 158.
(12) Olsen, A.; Roth, R. S. *J. Solid State Chem.* **1985**, *60*, 347.
(13) Ubic, R.; Reaney, I. M.; Lee, W. E. *J. Am. Ceram. Soc.* **1999**, *82* (5), 1336.
(14) Negas, T.; Yeager, G.; Bell, S.; Armen, R. In *Proceedings of the International Conference on the Chemistry of Electronic Ceramic Materials*, Jackson, WY, Aug 17−22, 1990; Davies, P. K., Roth, R. S., Eds.; p 21.

10.1021/cm020374m CCC: $22.00 
Published on Web 09/07/2002

composition of BaO 55 mol %, $Nd_2O_3$ 10 mol %, and $TiO_2$ 35 mol %. Its crystal structure was not resolved.[15] Further studies showed it to form with other rare earth elements: Y, Sm, Eu, Gd, Dy, Ho, Er, and Yb, for which we assigned the empirical formula $Ba_{12}R_{4.67}Ti_8O_{35}$ (R = rare earth elements). The X-ray diffraction, XRD, patterns, reported in JCPDS files (43-417 to 43-425), can be indexed with hexagonal unit cells. For R = Nd the lattice constants are $a \approx 5.99$ Å and $c \approx 29.96$ Å.

Previously, through study of superconducting $YBa_2Cu_3O_7$ films on $SrTiO_3$ substrates, Derks et al.[16] found a new Ba−Y−Ti−O phase at the interface. The bulk form of this phase was later produced by solid-state reaction of $YBa_2Cu_3O_7$ and $SrTiO_3$ powder. The XRD pattern was indexed on a hexagonal unit cell, $a = 5.928$ Å, $c = 29.514$ Å, and $Z = 4$. The space group $P6_3/mmc$ and the formula $Ba_3YTi_2O_{8.5}$ was assigned. This new phase was also confirmed by Chen et al.[17,18] A close examination showed $Ba_3YTi_2O_{8.5}$ and the $Q_1$ phases to have very similar XRD patterns, thereby implying the similar composition and structure and raising questions as to the correct formulas and detailed structure for these phases. Additionally, we have recently found[19] these materials exhibit mixed oxide-ion and hole conductivity. For R = Y, the bulk conductivity at 700 °C is $1.8 \times 10^{-3}\ \Omega^{-1}\ cm^{-1}$ and the oxygen transport number is about 0.35 over the temperature range 300−700 °C.

Determination of the crystal structure of this new class of rare-earth-containing barium titanates is essential for understanding the properties. In this paper, we report the structures for the Nd and Y members determined by X-ray and neutron powder diffraction, ND. Both have hexagonal 12-layer perovskite-related structure with space group $P6_3/mmc$. On the basis of the structure refinements, the formula $Ba_6R_2Ti_4O_{17}$ (or $Ba_3RTi_2O_{8.5}$, R = Nd and Y) was determined. In these structures, Nd and Y are octahedrally coordinated by oxygen; ordered oxygen vacancies are present in a pseudo-cubic [$BaO_2$] layer, resulting in tetrahedral coordination for Ti. The far-infrared spectra are consistent with the existence of titanate tetrahedra.

## 2. Experimental Section

Samples were prepared by conventional solid-state reaction at high temperature. Reagent-grade $BaCO_3$, $TiO_2$, $Nd_2O_3$, and $Y_2O_3$ were used as starting materials, which were first dried at 700 °C overnight, weighted out, mixed together using an agate mortar and pestle, and fired initially at 900 °C for a few hours to expel $CO_2$. The powder was reground, pressed into pellets, and refired at high temperatures for 2−3 days; the process of grinding, pelleting, and firing was repeated 2 or 3 times until the final products were obtained. The firing temperatures for the Nd and Y compounds were 1250 and 1500 °C, respectively.

Electron diffraction was carried out using a JEOL 2000 EX TEMSCAN transmission electron microscope. XRD data were collected using a Rigaku D/max 2000 X-ray diffractometer (Cu Kα radiation, graphite monochromator, 50 kV, 100 mA) over the $2\theta$ range 5−120°. Time-of-flight ND was carried out at room temperature using the Special Environment Powder Diffractometer (SEPD) at the Intense Pulsed Neutron Source of Argonne National Laboratory. The structural model was first constructed by direct methods using the program EXPO[20] and refined by Rietveld analysis using the program GSAS.[21] Far-infrared absorption spectra in the range of 1000−50 $cm^{-1}$ were recorded with a Nicolet Magna 750 Fourier transform instrument.

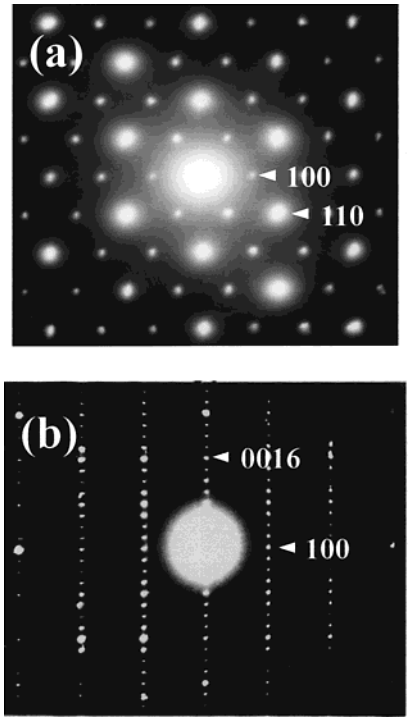


**Figure 1.** Electron diffraction patterns of $Ba_6Nd_2Ti_4O_{17}$: along the (a) [001] and (b) [110] directions.

## 3. Results and Discussion

**3.1. Electron Diffraction of $Ba_6Nd_2Ti_4O_{17}$.** From the electron diffraction patterns, $Ba_6Nd_2Ti_4O_{17}$ was tentatively assigned to a hexagonal unit cell with $a \approx 5.941$ Å and $c \approx 29.48$ Å. The patterns corresponding to the [001] and [100] directions are shown in Figure 1. On tilting, the patterns showed the systematic reflections, $00l$, $l = 2n$, which suggested the $P6_3$-type space groups, such as $P6_3/mmc$, $P6_3mc$, $P6_3/m$, and $P6_322$ as possible symmetries for this phase.

**3.2. Structure Determination of $Ba_6Nd_2Ti_4O_{17}$.** Following the results of electron diffraction, the highest symmetry space group $P6_3/mmc$ symmetry was chosen to construct a structural model by direct methods using XRD data. In general, XRD provides insufficient contrast to differentiate the Ba and Nd and is insensitive to light atoms such as oxygen. Only the positions of Ba/Nd and Ti can be determined accurately by the Program EXPO. Referring to the structure of hexagonal perovskite $BaTiO_3$[7] and considering the positions of Ba/Nd and Ti as well as the large $c$ parameter, a 12-layer structure of stacking [$BaO_3$] layers in the sequence of $(ccchcc)_2$ as the starting model (Figure 2) was constructed. The

(15) Zheng, C.; West, A. R. *Spec. Ceram. 9, Br. Ceram. Proc.* **1992**, *49*, 247.
(16) Derks, W. P. T.; Van Hal, H. A. M.; Langereis, C. *Physica C* **1988**, *156*, 62.
(17) Chen, A.; Zhi, Y.; Bao, Y.; Dai, X.; Jiang, Q. *J. Phys.: Condens. Matter* **1994**, *6*, 3553.
(18) Chen, A.; Zhuge, X.; Han, J.; Zhi, Y.; Zhi, Q.; Vilarinho, P. M.; Baptista, J. L. *J. Chin. Ceram. Soc. (Chin.)* **1996**, *24* (6), 712.
(19) Jing, X.; West, A. R. *Acta Phys.-Chim. Sin.* **2002**, *18* (7), 617.
(20) Altomare, A.; Carrozzini, B.; Cascarano, G.; Giacovazzo, C.; Guagliardi, A.; Moliterni, A. G. G.; Rizzi, R. *EXPO user's manual*; Inst. Di Ric. Per lo Sviluppo di Metodologie Cristallografiche, CNR.
(21) Larson, A. C.; Von Dreele, R. B. Report LAUR 86-748, Los Alamos National Laboratory, Los Alamos, NM, 1985.

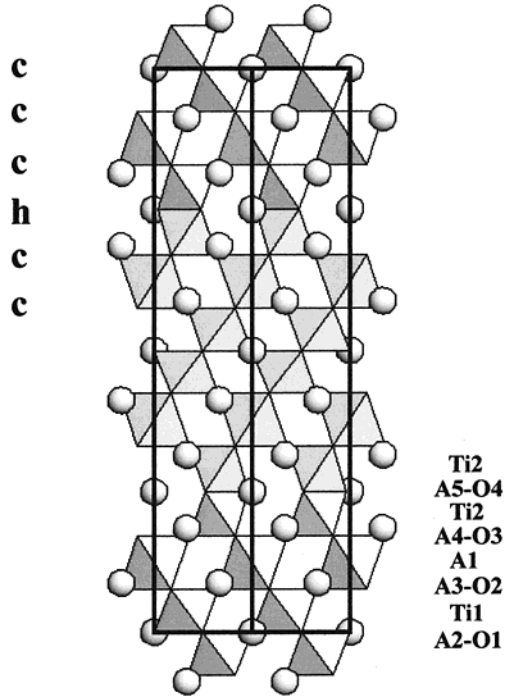


**Figure 2.** Projection of the initial structure model constructed for $Ba_6Nd_2Ti_4O_{17}$ by stacking $[BaO_3]$ layers according to sequence $(ccchcc)_2$ along the [110] direction.

possibility of oxygen vacancies was ignored at this stage. Among the five A positions for Ba and Nd atoms, A1 is 6-coordinate to oxygen and the others are 12-coordinate. Since $Nd^{3+}$ has a smaller ionic radius (1.123 Å)[22] than $Ba^{2+}$ (1.49 Å), we set Nd at the A1 position and Ba at the A2−A5 positions. Next, Rietveld analysis was attempted with oxygen atoms fixed in some assumed positions including the 6g and 12k and 6h sites. Initial refinement showed that atom O1 at site 6g (0.5, 0, 0) resulted in unphysically large thermal factors, which shed doubt on the assignment of this oxygen position. To determine the positions of O1, a Fourier difference map including all the atoms except atoms of O1 was calculated; Figure 3 shows the map at $z = 0$. Residue peaks were observed at 4f sites ($^1/_3$, $^2/_3$, 0), which implied the presence of oxygen at these sites instead of the 6g sites. One important consequence following the new oxygen position is that the Ba, O layer at $z = 0$ is not a close-packed layer $[BaO_3]$ but an oxygen-deficient layer $[BaO_2]$.

The next stage was to use ND to resolve those structural features that could not be satisfactorily determined by X-ray diffraction. The neutron scattering lengths[23] of Ba (5.25 fm), Nd (7.69 fm), and Ti (−3.30 fm) are significantly different, thus providing good resolving power among these atoms. Furthermore, the neutron scattering length of O (5.803 fm) is large so that the data are sensitive to oxygen locations. The refinements of ND data confirmed the location of Nd at the 6-coordinate A1 position and all the oxygen positional parameters. At the final stage, Rietveld refinements on both XRD and ND data were performed. During the refinement, the presence of impurity phases of $BaTiO_3$ and $Nd_2O_3$ with a concentration of about 1% was taken into account. The Rietveld profile fits of the diffraction data are shown in Figure 4 and final structural parameters listed in Table 1.

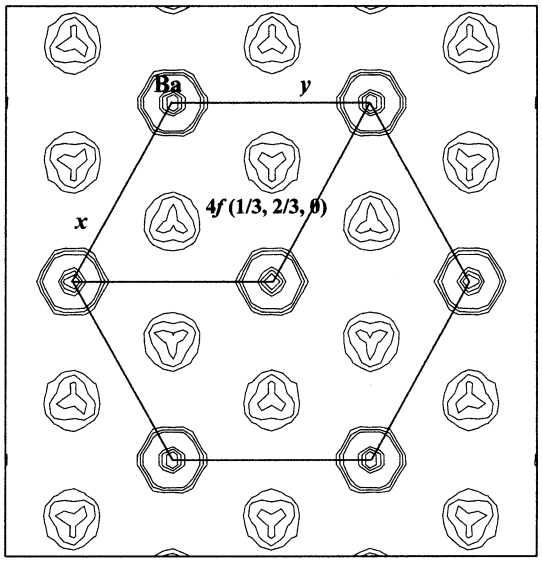


**Figure 3.** Calculated Fourier difference map at the $z = 0$ section with all the atoms except atoms of O1.

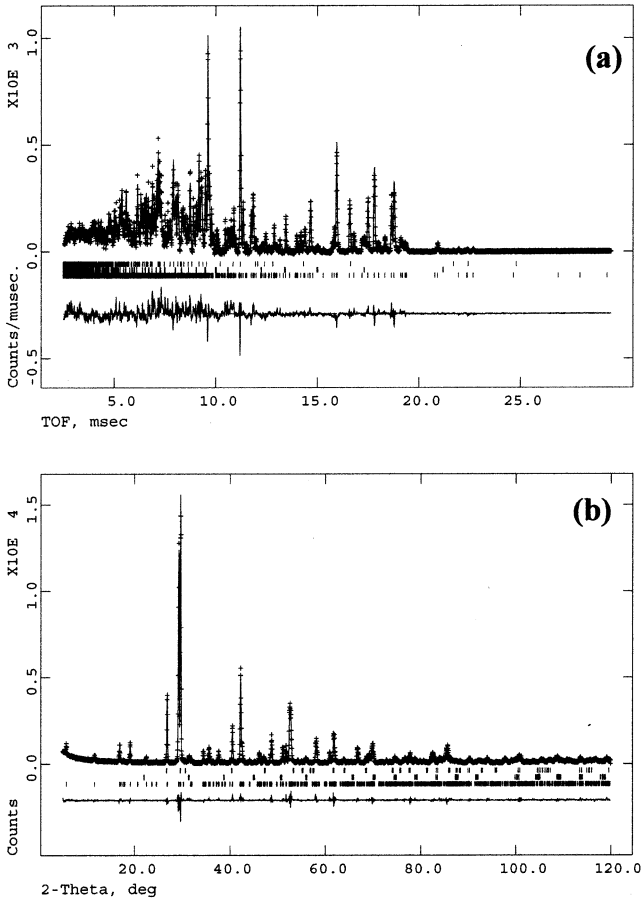


**Figure 4.** Rietveld profile fits of the neutron (a) and X-ray (b) powder diffraction data of $Ba_6Nd_2Ti_4O_{17}$. The three rows of vertical tick marks from bottom to top indicate the positions of Bragg reflections for the major $Ba_6Nd_2Ti_4O_{17}$ phase and minor impurity phases of $BaTiO_3$ and $Nd_2O_3$, respectively (the background in (a) was removed).

Figure 5 shows a projection of the structure of $Ba_6Nd_2Ti_4O_{17}$ along the [110] direction. It can be described

(22) Shannon, R. D. *Acta Crystallogr.* **1976**, *A32*, 751.
(23) Lovesey, S. W. *Theory of Neutron Scattering from Condensed Matter*; Clarendon Press: Oxford, 1984.

**Table 1. Refined Structural Parameters for $Ba_6Nd_2Ti_4O_{17}$[a]**

| atom | multiplicity | *x* | *y* | *z* | $U_{iso}$ (Å$^2$) |
|---|---|---|---|---|---|
| Nd | 4f | 0 | 0 | 0.12641(6) | 0.0023(4) |
| Ba1 | 2a | 0 | 0 | 0 | 0.055(2) |
| Ba2 | 4f | $^2/_3$ | $^1/_3$ | 0.08775(7) | 0.0070(5) |
| Ba3 | 4e | $^1/_3$ | $^2/_3$ | 0.18529(8) | 0.0058(5) |
| Ba4 | 2b | 0 | 0 | $^1/_4$ | 0.0050(8) |
| Ti1 | 4×c4 | $^1/_3$ | $^2/_3$ | 0.0527(2) | 0.007(1) |
| Ti2 | 4f | $^2/_3$ | $^1/_3$ | 0.2051(2) | 0.004(1) |
| O1 | 4f | $^1/_3$ | $^2/_3$ | −0.0039(3) | 0.068(2) |
| O2 | 12k | −0.3410(9) | −0.1705(5) | 0.0754(1) | 0.041(1) |
| O3 | 12k | 0.3564(6) | 0.1782(3) | 0.16999(9) | 0.0162(6) |
| O4 | 6h | 0.5220(3) | 0.0440(6) | $^1/_4$ | 0.0049(6) |

[a] Space group: $P6_3/mmc$; $a = 5.99283(9)$ Å, $c = 29.9289(8)$ Å; $Z = 2$; Rwp = 0.094, Rp = 0.064.

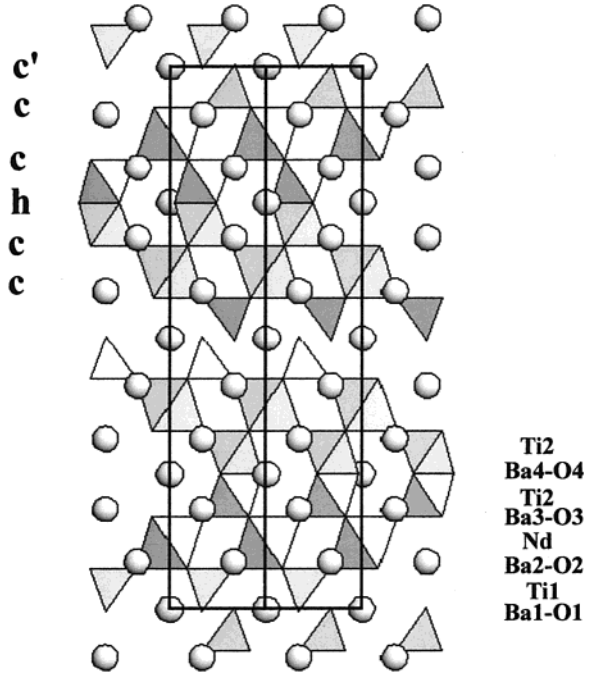


**Figure 5.** Projection of the final structure of $Ba_6Nd_2Ti_4O_{17}$ along the [110] direction.

as stacking cubic (c) and hexagonal (h) [$BaO_3$] layers with oxygen-deficient cubic (c′) [$BaO_2$] layers perpendicular to the *c* axis in the sequence $(c'cchcc)_2$. This structure accommodates face-sharing $TiO_6$ octahedral layers ($Ti_2O_9$), $NdO_6$ octahedral layers, and $TiO_4$ tetrahedral layers that appear in the [$BaO_2$] layers. In most Ti-containing oxide phases, Ti is present in $TiO_6$ octahedra; only a few compounds such as $Ba_2TiO_4$ show the $TiO_4$ tetrahedra.[24,25] In general, rare-earth ions having large ionic radii prefer higher (>7) oxygen coordination. In $Ba_6Nd_2Ti_4O_{17}$, the $RO_6$ (R = Nd) octahedral coordination is also uncommon, but does occur also in trigonal perovskite-related compounds $Ba_3R_4O_9$ (R = Gd to Lu).[26]

Tables 2 and 3 list the bond lengths and angles. The Ti−O bonds in $TiO_4$ tetrahedra vary between 1.70 and 1.82 Å and the O−Ti−O angles of the $TiO_4$ tetrahedra are within 107−112°, close to those observed in $Ba_2TiO_4$ (1.79−1.83 Å and 106−116°). The Ti−O bonds in $Ti_2O_9$ vary from 1.92 to 2.01 Å and those of Nd−O from 2.26 to 2.34 Å. The O−M−O angles in $MO_6$ octahedra (M = Ti or Nd) are within 80−94°. Table 2 also lists the sums of bond valences, $\sum V_{i-j}$, calculated by using Brown's method.[27] The sums of bond valences for Ti1, Ti2, and all the oxygen atoms are in reasonable agreement with the valence sum rule, while those for Nd and all the Barium atoms have some deviations. These deviations are probably due to the particular character of this structure: the existence of $NdO_6$ octahedra and [$BaO_2$] layers (or $TiO_4$ tetrahedra).

**Table 2. Bond Lengths and Sums of Bond Valences for $Ba_6Nd_2Ti_4O_{17}$**

| | | | |
|---|---|---|---|
| Nd−O2 (×3) | 2.338(4) Å | Ba3−O3 (×6) | 3.0341(5) Å |
| Nd−O3 (×3) | 2.263 (3) Å | Ba3−O4 (×3) | 2.754(3) Å |
| ($\sum V_{Nd-O}$ = 3.555) | | ($\sum V_{Ba3-O}$ = 1.641) | |
| Ba1−O1 (×6) | 3.4620 (3) Å | Ba4−O3 (×6) | 3.026(3) Å |
| Ba1−O2 (×6) | 2.867(4) Å | Ba4−O4 (×6) | 3.0051(3) Å |
| ($\sum V_{Ba1-O}$ = 1.494) | | ($\sum V_{Ba4-O}$ = 1.668) | |
| Ba2−O1 (×1) | 2.508(8) Å | Ti1−O1 (×1) | 1.70(1) Å |
| Ba2−O2 (×6) | 3.0196(5) Å | Ti1−O2 (×3) | 1.821(5) Å |
| Ba2−O3 (×3) | 2.941(4) Å | ($\sum V_{Ti1-O}$ = 4.331) | |
| ($\sum V_{Ba2-O}$ = 1.897) | | Ti2−O3 (×3) | 1.923(4) Å |
| | | Ti2−O4 (×3) | 2.016(4) Å |
| | | ($\sum V_{Ti2-O}$ = 3.984) | |
| | $\sum V_{i-j}$ | | $\sum V_{i-j}$ |
| O1 | 2.052 | O3 | 1.968 |
| O2 | 1.998 | O4 | 2.010 |

**Table 3. Bond Angles of O−M-O in Polyhedra for $Ba_6Nd_2Ti_4O_{17}$**

| bond | bond angle (deg) | bond | bond angle (deg) |
|---|---|---|---|
| O2−Nd−O2 (×3) | 81.9(2) | O3−Ti2−O3(×3) | 93.0(2) |
| O2−Nd−O3 (×6) | 93.87(7) | O3−Ti2−O4(×6) | 93.01(8) |
| O3−Nd−O3 (×3) | 90.1(1) | O4−Ti2−O4(×3) | 80.4(2) |
| O1−Ti1−O2 (×3) | 111.8(2) | | |
| O2−Ti1−O2 (×3) | 107.0(2) | | |

**Table 4. Refined Structural Parameters for $Ba_6Y_2Ti_4O_{17}$[a]**

| atom | multiplicity | *x* | *y* | *z* | $U_{iso}$ (Å$^2$) |
|---|---|---|---|---|---|
| Y | 4f | 0 | 0 | 0.12687(6) | 0.0043(3) |
| Ba1 | 2a | 0 | 0 | 0 | 0.046(1) |
| Ba2 | 4f | $^2/_3$ | $^1/_3$ | 0.08815(5) | 0.0063(4) |
| Ba3 | 4e | $^1/_3$ | $^2/_3$ | 0.18285(5) | 0.0063(4) |
| Ba4 | 2b | 0 | 0 | $^1/_4$ | 0.0043(5) |
| Ti1 | 4f | $^2/_3$ | $^1/_3$ | −0.0549 (1) | 0.0070(9) |
| Ti2 | 4f | $^2/_3$ | $^1/_3$ | 0.2039(1) | 0.0011(7) |
| O1 | 4f | $^1/_3$ | $^2/_3$ | −0.0041(2) | 0.071(2) |
| O2 | 12k | −0.3378(7) | −0.1689(3) | 0.07797(8) | 0.0266(5) |
| O3 | 12k | 0.3510(5) | 0.1755(3) | 0.16875(6) | 0.0124(4) |
| O4 | 6h | 0.5212(3) | 0.0424(5) | $^1/_4$ | 0.0042(4) |

[a] Space group: $P6_3/mmc$; $a = 5.93055(4)$ Å, $c = 29.5239$ (3) Å; $Z = 2$; Rwp = 0.092, Rp = 0.060.

**3.3. Structural Determination of $Ba_6Y_2Ti_4O_{17}$.** The determination of the $Ba_6Y_2Ti_4O_{17}$ structure followed closely the procedure for $Ba_6Nd_2Ti_4O_{17}$, as described in a previous section. Since both Y and Nd are trivalent and have similar ionic radius and electronegativity, it is not surprising that $Ba_6Y_2Ti_4O_{17}$ are isostructural to $Ba_6Nd_2Ti_4O_{17}$. The structure parameters for $Ba_6Y_2Ti_4O_{17}$ obtained from Rietveld refinements of the X-ray and neutron data are given in Table 4. Tables 5 and 6 list the bond lengths along with the corresponding sums of bond valences and bond angles of O−M−O in $MO_6$ octahedra (M = Ti or Y) and $TiO_4$ tetrahedra, respectively.

(24) Wu, K. K.; Brown, I. D. *Acta Crystallogr.* **1973**, *B29*, 2009.
(25) Günter, J. R.; Jameson, G. B. *Acta Crystallogr.* **1984**, *C40*, 207.
(26) Müller-Buschbaum, Hk.; Schrandt, O. *J. Alloys Compd.* **1993**, *191*, 151.
(27) Brown, I. D.; Altermatt, D. *Acta Crystallogr.* **1985**, *B41*, 244.

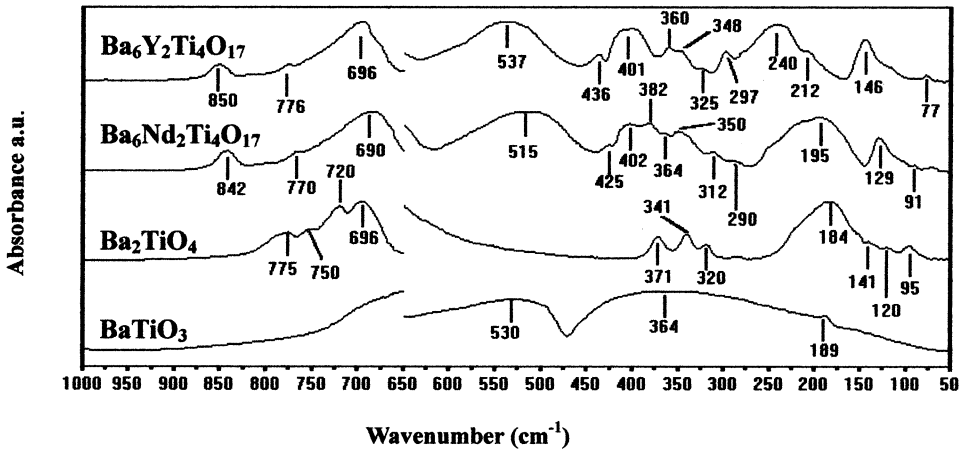


**Figure 6.** Far-infrared absorption spectra for $Ba_6Nd_2Ti_4O_{17}$, $Ba_6Y_2Ti_4O_{17}$, $BaTiO_3$, and $Ba_2TiO_4$.

**Table 5. Bond Lengths and Sums of Bond Valences for $Ba_6Y_2Ti_4O_{17}$**

| | | | |
|---|---|---|---|
| Y−O2 (×3) | 2.257(3) Å | Ba3−O3 (×6) | 2.9958(4) Å |
| Y−O3 (×3) | 2.186(3) Å | Ba3−O4 (×3) | 2.767(2) Å |
| ($\Sigma V_{Y-O}$ = 3.489) | | ($\Sigma V_{Ba3-O}$ = 1.701) | |
| Ba1−O1 (×6) | 3.4262(2) Å | Ba4−O3 (×6) | 3.001(2) Å |
| Ba1−O2 (×6) | 2.883(3) Å | Ba4−O4 (×6) | 2.9732(2) Å |
| ($\Sigma V_{Ba1-O}$ = 1.470) | | ($\Sigma V_{Ba4-O}$ = 1.806) | |
| Ba2−O1 (×1) | 2.481(7) Å | Ti1−O1 (×1) | 1.743(8) Å |
| Ba2−O2 (×6) | 2.9806(3) Å | Ti1−O2 (×3) | 1.821(4) Å |
| Ba2−O3 (×3) | 2.879(3) Å | ($\Sigma V_{Ti1-O}$ = 4.167) | |
| ($\Sigma V_{Ba2-O}$ = 2.110) | | Ti2−O3 (×3) | 1.925(3) Å |
| | | Ti2−O4 (×3) | 2.022(3) Å |
| | | ($\Sigma V_{Ti2-O}$ = 3.945) | |
| | $\Sigma V_{i-j}$ | | $\Sigma V_{i-j}$ |
| O1 | 1.942 | O3 | 2.020 |
| O2 | 2.015 | O4 | 2.004 |

**Table 6. Bond Angles of O−M−O in Polyhedra for $Ba_6Y_2Ti_4O_{17}$**

| bond | bond angle (deg) | bond | bond angle (deg) |
|---|---|---|---|
| O2−Y−O2 (×3) | 83.5(1) | O3−Ti2−O3 (×3) | 93.7(1) |
| O2−Y−O3 (×6) | 92.57(5) | O3−Ti2−O4 (×6) | 92.97(6) |
| O3−Y−O3 (×3) | 91.2(1) | O4−Ti2−O4 (×3) | 79.6(1) |
| O1−Ti1−O2 (×3) | 112.0(1) | | |
| O2−Ti1−O2 (×3) | 106.9(1) | | |

**3.4. Far-Infrared Spectroscopy.** To provide further evidence of the presence of $TiO_4$ tetrahedra in $Ba_6R_2Ti_4O_{17}$ (R = Nd and Y), far-infrared absorption spectra were collected at room temperature. The data were compared with two reference spectra, for $Ba_2TiO_4$, which contains $TiO_4$ tetrahedra, and $BaTiO_3$, which contains $TiO_6$ octahedra, in Figure 6. The spectra were separately recorded in two wavenumber ranges, 1000−650 and 650−50 $cm^{-1}$; thus, the baseline is not continuous near 650 $cm^{-1}$.

The infrared spectroscopy of tetragonal $BaTiO_3$ was investigated by Last[28] and Spitzer et al.[29] Three absorption bands were reported: 600−500 $cm^{-1}$ for the Ti−O stretching modes, 400−350 $cm^{-1}$ for the Ti−O bending modes in $TiO_6$,[28] and 200−100 $cm^{-1}$ for the mode of Ba−$TiO_6$.[29] For $Ba_2TiO_4$, according to Wijzen et al.,[30] there are two bands, around 700 and 350 $cm^{-1}$, corresponding to the stretching and bending modes of $TiO_4$ tetrahedra, respectively. The spectra of $BaTiO_3$ and $Ba_2TiO_4$ in Figure 6 agree well with the previous reports.[28−30] The spectra of $Ba_6R_2Ti_4O_{17}$ are more complex, probably due to the existence of $TiO_4$, $RO_6$, and $TiO_6$ structural units and exhibit four absorption bands: 900−650, 650−500, 500−200, and 200−50 $cm^{-1}$. The band at 600−500 $cm^{-1}$ could be attributed to the stretching modes of Ti−O in $TiO_6$ and/or R−O in $RO_6$, that at 200−50 $cm^{-1}$ to Ba−$TiO_6$ (and/or $RO_6$) and/or Ba−$TiO_4$, that at 900−650 $cm^{-1}$ to Ti−O stretching modes in tetrahedra $TiO_4$, and that at 500−200 $cm^{-1}$ to Ti−O bending mode in $TiO_4$ and $TiO_6$ (and/or $RO_6$).

## 4. Summary

The crystal structures of $Ba_6Nd_2Ti_4O_{17}$ and $Ba_6Y_2Ti_4O_{17}$ were investigated by electron, X-ray, and neutron diffraction and infrared absorption spectroscopy. The combined XRD and ND data permit refinement of the full structure using the Rietveld method. Both materials exhibit a hexagonal 12-layer perovskite-related structure. The stacking sequence of the cubic (c), hexagonal (h), and oxygen-deficient pseudo-cubic (c′) perovskite layers according to $(c'cchcc)_2$ was identified. The oxygen-deficient closed-packed $[BaO_2]$ layers permit the formation of $TiO_4$ tetrahedra layers. In both materials, Nd and Y are located on 6-coordinate sites.

**Acknowledgment.** Financial support from the Natural Science Foundation of China (20071003), Scientific Foundation for Returned Overseas Chinese Scholars, and Foundation for University Key Teacher by the Ministry of Education are gratefully acknowledged. We thank Prof. Jianhua Lin for invaluable discussions and S. M. Short for her help in the neutron experiment. Work performed at Argonne is supported by U.S. DOE-BES under Contract W-31-109-ENG-38.

CM020374M

(28) Last, J. T. *Phys. Rev.* **1957**, *105*, 1740.
(29) Spitzer, W. G.; Miller, R. C.; Kleinman, D. A.; Howarth L. E. *Phys. Rev.* **1962**, *126*, 1710.
(30) Wijzen, F.; Rulmont, A.; Tarte, P. *Spectrochim. Acta* **1994**, *50A*, 677.